Tellus (2006), 58A, 320–330
Printed in Singapore. All rights reserved

TELLUS

22 views of the global albedo—comparison between 20 GCMs and two satellites

By FRIDA A-M. BENDER[1]*, HENNING RODHE[1], ROBERT J. CHARLSON[2], ANNICA M. L. EKMAN[1] and NORMAN LOEB[3], [1]*Department of Meteorology, Stockholm University, S-10691 Stockholm, Sweden;* [2]*Department of Atmospheric Sciences, University of Washington, Seattle, USA;* [3]*Department of Atmospheric Science, Hampton University, Hampton, USA*

(Manuscript received 13 October 2005; in final form 17 January 2006)

ABSTRACT

A comprehensive comparison of characteristics of the planetary albedo (α) in data from two satellite measurement campaigns (ERBE and CERES) and output from 20 GCMs, simulating the 20th-century climate, is performed. Discrepancies between different data sets and models exist; thus, it is clear that conclusions about absolute magnitude and accuracy of albedo should be drawn with caution. Yet, given the present calibrations, a bias is found between different estimates of α, with modelled global albedos being systematically higher than the observed. The difference between models and observations is larger for the more recent CERES measurements than the older ERBE measurements. Through the study of seasonal anomalies and space and time distribution of correaltions between models and observations, specific regions with large discrepancies can be identified. It is hereby found that models appear to over-estimate the albedo during boreal summer and under-estimate it during austral summer. Furthermore, the seasonal variations of albedo in subtropical areas dominated by low stratiform clouds, as well as in dry desert regions in the subtropics, seem to be poorly simulated by the models.

1. Introduction

At the top of the atmosphere, there is an approximate balance between incoming and outgoing radiation, given by

$$0 \approx C\frac{\partial T_{\text{eff}}}{\partial t} = \pi R^2 S(1-\alpha) - 4\pi R^2 \sigma {T_{\text{eff}}}^4. \quad (1)$$

Here, the first term on the right represents the incident solar radiation, of which the fraction α, known as the planetary albedo, is reflected back to space. The second term represents the outgoing long-wave radiation, with its Stefan–Boltzmann dependence on the effective radiative temperature T_{eff}. C represents the Earth's total heat capacity, S the solar constant, R the Earth's radius and σ the Stefan–Boltzmann constant.

At a particular time and place, the approximate equality does not hold-local radiative imbalances is what drives the large-scale atmospheric and oceanic circulation—but for the global mean on a long time scale with a non-drifting T_{eff}, it must be true.

The planetary albedo thus plays a major role in the global energy budget, together with the solar constant and the outgoing long-wave radiation. For the energy fluxes to remain balanced, variability in albedo must correspond to variations in effective radiative temperature, and vice versa. In view of the relative stability of the climate during the Holocene, with global mean surface temperature (T_{surf}) varying within a range of ca. 1 K (IPCC, 2001; Moberg et al., 2005), it is reasonable to believe that the effective radiative temperature of the planet has remained stable as well. Obviously, neither T_{eff} and T_{surf}, nor the variations in the two are directly comparable. Amplification of surface temperature variability with altitude in the tropics, as given by models and measurements, is discussed by Santer et al. (2005). They conclude that month-to-month variability, and most likely also multi-decadal trends, are larger in tropospheric temperature than in surface temperature, by a factor of no more than three. Even assuming an amplification of this order of magnitude, a 1 K variation in T_{surf} corresponds to a ca. 0.01 variation in α, according to eq. (1).

We are hence led to believe that the planetary albedo also has remained stable during the Holocene. This is remarkable since the albedo is highly dependent on clouds, which exhibit large variability in space and time. Therefore numerous questions arise; What might cause this stability? What kind of processes and feedbacks may be involved and have the conditions for them changed during the industrial era? Can the stability be disturbed by human impact or is the system resilient? To address questions of this kind it is necessary to have a clear

*Corresponding author.
e-mail: frida@misu.su.se
DOI: 10.1111/j.1600-0870.2006.00181.x

understanding of the planetary albedo itself, and its spatial and temporal variability.

Hitherto there has been a lack of consensus on the trends and variabilty of the large-scale albedo. Wielicki et al. (2002) examined the variability in the radiative energy budget, including albedo, in the tropics and related satellite-inferred variability to variable tropical cloudiness. Global albedo was addressed by Wielicki et al. (2005), who showed that satellite measurements contradict estimates of albedo changes from near-global earthshine observations (Pallé et al., 2004), that is, measurements of the light reflected back to Earth from the dark side of the moon.

There also remains uncertainty in estimating the absolute magnitude of global albedo. The largest source of uncertainty arises from the difficulties with absolute calibration of current state-of-the-art instruments.

The albedo is governed by surface properties (land use, vegetation type and the extent of snow and ice sheets), clouds (cloud cover and radiative properties of clouds) as well as atmospheric aerosols. Each of these factors and their effects on the albedo and the radiative balance can be and have been studied separately. This is especially true for radiative effects of clouds and cloud-type variations. To mention only some; Roeckner et al. (1987), Ramanthan et al. (1989), Harrison et al. (1990), Charlson et al. (1992) Hartmann et al. (1992), Chen et al. (2000) and Potter and Cess (2004).

We choose instead to study the albedo as an integrative factor. We evaluate all-sky fluxes (not distinguishing between clear and cloudy skies) at the top of the atmosphere, and thereby estimate the total reflective properties of the surface and atmosphere system all at once, letting individual factors enter into the global albedo picture in a secondary way.

The main source of global top-of-the-atmosphere radiative flux data is satellite measurements. But observations are sparse and associated with errors and uncertainties, which causes apparent disagreement. Non-overlapping measurements and gaps in time series is a critical problem. As a complement to observations, physically based models can be a powerful tool for gaining understanding of the climate system. Of course, models as well have errors and uncertainties, and cannot either claim to represent 'the truth'. With two imperfect sources, consistency is a necessary but insufficient condition for defining absolute accuracy and, in lack of absolute and accurate estimates of albedo, agreement between models and measurements is desired.

In an attempt to bridge the gap between models and measurements and to survey the currently available characterizations of global albedo, we carry out a systematic comparison between the albedo output from an ensemble of GCMs presently in use for present-day as well as future climate simulations, and satellite observations of global albedo from the mid-1980s to the early 2000s, through the ERBE and CERES campaigns (to be described in Section 2) .

We study absolute values (Section 3.1), seasonal cycles (Section 3.2), trends (Section 3.3) and spatial and temporal distribution of agreement (Sections 3.4 and 3.5) of albedo in models and satellite measurements. The present study is aimed at providing an insight into how the prevailing views of the global albedo differ. By pointing out and quantifying differences, we hope to inspire both modellers and experimentalists to refine their products. The analysis we perform is a necessary first step towards solving the climate stability puzzle.

2. Data sets and model output

In this study, there are two main sources of information—calculations from satellite-borne radiometers and GCM output.

Data from the Earth Radiation Budget Experiment (ERBE) (Barkstrom, 1984; Barkstrom and Smith, 1986) and the Clouds and the Earth's Radiant Energy System (CERES) (Wielicki et al., 1996; Smith et al., 2004) are used. ERBE instruments have been placed on the ERBS, NOAA-9 and NOAA-10 satellites, and CERES instruments are still in operation on Terra and Aqua, and were previously operating on TRMM, measuring top-of-the-atmosphere (henceforth, referred to as TOA) radiative fluxes. Here, monthly means of SW (short-wave) fluxes are used to calculate monthly mean albedo.

As seen in Table 1, the ERBE observations studied cover a time period from November 1984 to February 1990, with global coverage between February 1985 and May 1989, and the CERES observations utilized cover the period March 2000 to December 2003.

The CERES and ERBE products studied here are not only derived from different instruments with different resolutions, sampling modes and orbits, but also based on very different algorithms for scene identification, angular distribution models and directional models etc., and their absolute levels are therefore not strictly comparable. Further information on uncertainties and data set differences can be found in project documentations and data quality summaries on the NASA website (from http://eosweb.larc.nasa.gov). An additional data set of ERBE-like CERES observations, based on the ERBE algorithms, is available and should be used when studying long-term trends in radiative fluxes, but in our comparison with model ouput, we choose to use a recently developed and more refined CERES product.

The albedo error estimates given in Table 1 are based on the estimates of errors in monthly mean SW radiative fluxes given by Wielicki et al. (1995). The SW flux errors are converted into albedo errors through error propagation calculations. The total error is a combination of a bias or calibration error and a random or precision error (from angle sampling, space sampling and time sampling).

The model output used is obtained from coordinated simulations with 20 different coupled ocean-atmosphere GCMs, performed in support of the IPCC Fourth Assessment Report. We use modelled incoming and outgoing SW radiation at the top of the atmosphere, given as monthly mean values on grids of

Table 1. Data used in the present study[a]

	Time	Satellite	Grid	Coverage	tot. err.	Bias	rand. err.
ERBE	Nov 84–Feb 90	ERBS	$2.5^\circ \times 2.5^\circ$	67.5°N − 67.5°S	0.017	0.0064	0.016
ERBE	Feb 85–Jan 87	NOAA-9	$2.5^\circ \times 2.5^\circ$	global	0.017	0.0064	0.016
ERBE	Nov 86–May 89	NOAA-10	$2.5^\circ \times 2.5^\circ$	global	0.017	0.0064	0.016
CERES	Mar 00–Dec 03	Terra	$1^\circ \times 1^\circ$	global	0.0077	0.0031	0.0031

[a]Time periods covered by different satellites, the horizontal resolution and the spatial coverage are specified. The errors are given as one standard deviation according to Wielicki et al. (1995). The ERBE data are the official ERBE S-4G Scanner data set, obtained from the Atmospheric Sciences Data Center at NASA Langley Research Center. The CERES TOA fluxes are derived from instantaneous TOA fluxes on the CERES Terra Edititon2B Rev1 Single Scanner Footprint TOA/Surface Fluxes and Clouds (SSF) product (Loeb et al., 2005), converted by application of diurnal albedo models derived from Angular Distribution Models (ADMs) according to Loeb et al. (2003). These CERES data have also been corrected for spectral darkening, and are therefore not afflicted with the spurious trend discussed by Wielicki et al. (2005).

varying spatial resolution. The simulations are based on historical changes in forcings, and cover a time period from the mid-19th century to ca. 2000, the end date for the simulations varying between different models. The forcing agents included in the simulations also vary somewhat, but the effects of the differences are considered unimportant for our purposes of comparison. All models include varying greenhouse gas (GHG) levels and sulfate aerosol burdens. Some of the simulations include only anthropogenic forcing, while most also include the appropriate solar and volcanic variability. The models, with abbreviations, are listed in Table 2. Note that the simulations and the set of models, differ from those in the AMIP projects (Gates and Boyle, 1992; Gates et al., 1999), which have been used in studies by for example, Weare (2004) and Potter and Cess (2004).

3. Comparison between models and measurements

3.1. General characteristics

The ERBE-measured range and geographical distribution of albedo is described by for example, Harrison et al. (1990) and Ramanthan et al. (1989). The models are roughly able to capture these general characteristics. They have a similar range of albedos, the monthly mean ratio between incident and reflected SW radiation at each grid point varying between ca. 0.1 and 0.8. The lowest values are found over low-latitude ocean areas, and the highest values are found at the snow- and ice-covered high northern latitudes. High values due to snow also appear at lower latitudes over mountain areas. The albedo is generally higher over the continents than over the oceans. The great impact of clouds on the albedo has been made evident by the comparison between clear-sky and all-sky albedo in Harrison et al. (1990).

In Figure 1, we compare the global mean time series for the 20 models (February 1985–ca. 2000) with ERBE (February 1985–May 1989) and CERES (March 2000–December 2003) observations. The global mean albedos are calculated as the ratio between the geographically weighted global monthly mean incident SW radiation and the similarly weighted and averaged reflected SW radiation. There is a spread in the modelled time series, the mean albedos ranging from 0.294 in GISS-EH to 0.319 in CNRM-CM3. ERBE is at the lower end of the model span, with a mean albedo of 0.2942 ± 0.006, and CERES is even lower, with a mean of 0.282 ± 0.003. The uncertainties here refer to the calibration errors or biases in the measurements (cf. Section 2). The average of the modelled global mean albedos is ca. 0.009 higher than the ERBE estimate of the same quantity and ca. 0.02 higher than the CERES estimate. Translated into SW flux anomaly, in accordance with Wielicki et al. (2005), these differences correspond to 3.0 Wm^{-2} and 6.8 Wm^{-2}, respectively. This can be compared to the frequently used reference point of a 2.4-Wm^{-2} radiative forcing due to anthropogenic GHG (IPCC, 2001). The present accuracy for albedo inferences is thus insufficient. To judge the importance of albedo variations and changes, relative to anthropogenic forcings relevant to the climate change discussion, the accuracy would need to be roughly an order of magnitude better.

As discussed in Section 2, the absolute albedo levels of the two observational data sets may not be directly comparable (see online data quality summaries at http://eosweb.larc.nasa.gov). The difference between them should not necessarily be interpreted as an indication of a drop in global mean albedo. There are, however, other observations that point towards a decrease in albedo over the past decades—melting of sea ice and shortened snow cover extent in the Arctic (ACIA, 2004) and decreasing total cloud amount (Norris, 2005) for instance.

The models do not show a difference between the late 1980s and the early 2000s, and remain closer to the ERBE values. None of the model means are within the given uncertainty range for the CERES mean, and only GISS-ER, GISS-EH, MIORC3.2(hires), MRI-CGCM2.3.2, UKMO-HadCM3 and UKMO-HadGEM1 are within the uncertainty range for the ERBE mean (again using the calibration part of the uncertainty).

The difference between the two measurement sets illustrates the insufficient accuracy of albedo levels that currently

Table 2. Models used in the present study[a]

Modelling group(s)	Country	IPCC ID	ATM. Resolution
Bjerknes Center for Climate Research	Norway	BCCR-BCM2.0	2.8° × 2.8°, L31
Canadian Centre for Climate Modelling and Analysis	Canada	CGCM3.1	3.8° × 3.8°, L31
Center for Climate System Research (The University of Tokyo), National Institute for Environmental Studies, and Frontier Research Center for Global Change (JAMSTEC)	Japan	MIROC3.2(hires)	1.1° × 1.1°, L56
		MIROC3.2(medres)	2.8° × 2.8°, L20
CSIRO Atmospheric Research	Australia	CSIRO-Mk3.0	1.9° × 1.9°, L18
Hadley Centre for Climate Prediction and Research/Met Office	United Kingdom	UKMO-HadCM3	3.8° × 2.5°, L19
		UKMO-HadGEM1	1.9° × 1.3°, L38
Institut Pierre Simon Laplace	France	IPSL-CM4	3.8° × 2.5°, L19
Institute for Numerical Mathematics	Russia	INM-CM3.0	5.0° × 4.0°, L21
LASG/Institute of Atmospheric Physics	China	FGOALS-g1.0	2.8° × 3.0°, L26
Max Planck Institute for Meteorology	Germany	ECHAM5/MPI-OM	1.9° × 1.9°, L31
Meteo-France, Centre National de Recherches Meteorologiques	France	CNRM-CM3	2.8° × 2.8°, L45
Meteorological Institute of the University of Bonn, Meteorological Research Institute of KMA, and Model and Data group	Germany/Korea	ECHO-G	3.8° × 3.8°, L19
Meteorological Research Institute	Japan	MRI-CGCM2.3.2	2.8° × 2.8°, L30
NASA/Goddard Institute for Space Studies	USA	GISS-EH	3.9° × 5.0°, L20
		GISS-ER	3.9° × 5.0°, L20
National Center for Atmospheric Research	USA	CCSM3	1.4° × 1.4°, L28
		PCM	2.8° × 2.8°, L26
US Dept. of Commerce/NOAA/Geophysical Fluid Dynamics Laboratory	USA	GFDL-CM2.0	2.5° × 2.0°, L24
		GFDL-CM2.1	2.5° × 2.0°, L24

[a]More detailed model documentation can be found at the PCMDI-website (www-pcmdi.llnl.gov/ipcc/model˙documentation/ipcc˙model˙documentation.php). The resolutions given correspond to the Gaussian grid on which the atmospheric output is delivered.

available measurements can supply, and is interesting from a tuning standpoint. Obviously, tuning levels of model TOA fluxes to either measurement set will lead to disagreement with the other. Presently, the atmospheric components of coupled models are commonly tuned to ERBE, which can be exemplified by the NCAR CCM3, in which the global annual mean TOA fluxes are tuned to agree with ERBE (Kiehl et al., 1998).

The seasonal variation of albedo is large in the models as well as the observations, and the comparison between models and measurements is largely dominated by this feature. In order to discern and to study variations that are not linked to seasons, for example, trends and year-to-year variations, we de-seasonalize the data, that is, we study the anomalies between month i and the mean of all months i in the measurement period, for $i =$ January, . . . , December. The annual cycle of albedo is discussed in more detail in Section 3.2.

Figure 2 shows boxplots for global mean albedo in the models and the observations. The models and ERBE cover the same time

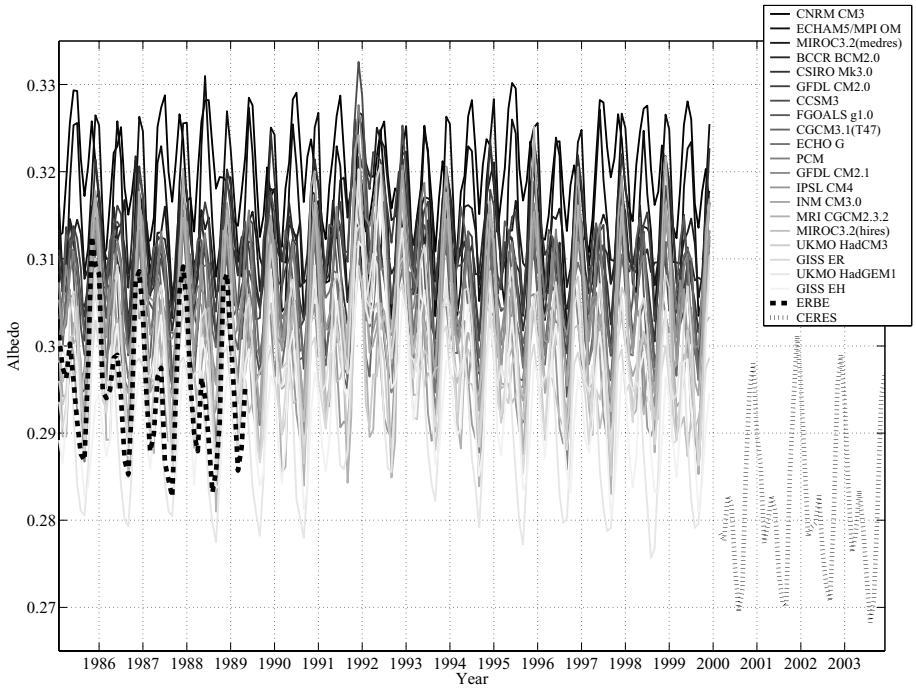

Fig. 1. Global monthly mean albedo time series from 20 GCMs (solid grey lines) compared with ERBE and CERES satellite observations (dashed black lines).

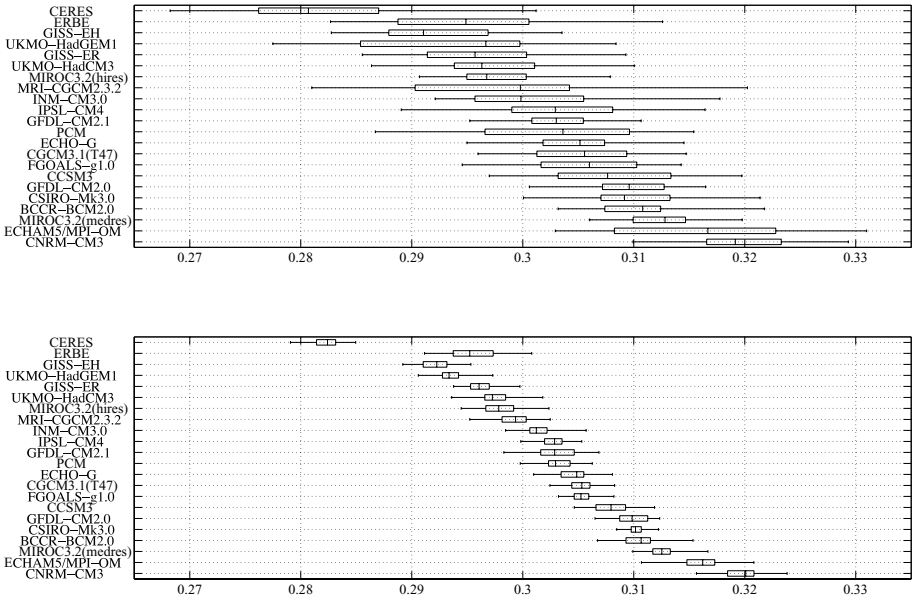

Fig. 2. Boxplots for global monthly mean albedo in CERES (March 2000–December 2003), ERBE and 20 models (all February 1985–May 1989). Minimum and maximum values, upper and lower quartiles and median values are indicated. Upper panel: Seasonal cycle included; Lower panel: de-seasonalized time series.

period (February 1985–May 1989), whereas CERES covers the period from March 2000 to December 2003.

The models are sorted by ascending median global mean albedo, and it is once again evident that there is a spread in the models and that ERBE is at the lower end of the span, and CERES even lower. The spread in each series, indicated by the inter-quartile range and the total range in the plots, is largely due to the seasonal cycle, which is included in the upper panel of Fig. 2. Here, the ranges vary somewhat between the different time series but the observations do

not stand out as having larger or smaller variation than the models.

In the lower panel of Fig. 2, the time series are de-seasonalized. This decreases the spread in the data, it now only being due to year-to-year variations. ERBE is here seen to have a larger spread, and thereby a larger year-to-year variation, than CERES and any of the models. This is to a large extent an effect of the trend in the ERBE data (cf. Section 3.3).

In the discussion of Fig. 2, it should also be remembered that the CERES data are not from the same time period as the ERBE data and the model output. Therefore, for instance, the variability in the ERBE data might be greater than that in the CERES data since the ERBE period includes both the 1987 El Niño and the 1989 La Niña, whereas CERES captures only the weak 2002 El Niño.

3.2. Annual cycle

In Figure 3, we compare the annual cycles of albedo for the model simulations ERBE and CERES.

Annual cycles of albedo anomalies from ERBE and CERES agree well, although the absolute values in the two data sets are different (as discusssed in Section 3.1).

Both ERBE and CERES have clearly double-peaked global mean seasonal cycles, with a higher peak around the Northern Hemisphere (NH) winter solstice (November–January) and a lower peak around the NH summer solstice (May–June). The differences between summer and winter maxima are 0.011 and 0.017 for ERBE and CERES, respectively. The bimodal character of the annual cycle is likely linked to the snow and ice cover at the sunlit high latitudes—both polar areas have very high albedos when they are illuminated, giving rise to two peaks per year. In the Southern Hemisphere (SH), the high-albedo area seems to be small enough not to be sunlit during austral winter, whereas in the NH there is an area of very high albedo all year round. This could be a cause of the higher peak during boreal winter, when high albedos in both polar areas contribute to the global mean. Similarly, the SH also has a more pronounced seasonal cycle than the NH (not shown).

The models do quite well in capturing the seasonal cycle in global mean albedo, and the modelled monthly anomalies differ only slightly from those observed by satellites. The models do not capture the difference in amplitude between the two local maxima, and have a more even seasonal cycle, underestimating the albedo during austral summer and overestimating the albedo during boreal summer, compared to the observations. The difference between the summer and winter peaks in the models is less than half of that in the measurements (ca. 0.005). The largest discrepancy between models and measurements appears at the boreal winter maximum, possibly indicating that the models have difficulties especially with the snow and ice cover in the SH polar regions. Of course, there is also the possibility that poor cloud simulations cause the discrepancies. In Section 3.5, we see further indication that the models under-estimate the high southern latitude albedo during boreal winter. According to Fig. 3, the modelled boreal summer maximum does not deviate so much from the observed values, but this maximum appears a little later, and is broader in the models than in the measurements.

3.3. Temporal trends

As mentioned in Section 1, there is disagreement regarding the trends in global albedo over the past decades. In light of this, it is interesting to find that none of the models show statistically significant trends over the period from 1985 to 2000. Hence, in the GCM simulations neither the natural nor the anthropogenic

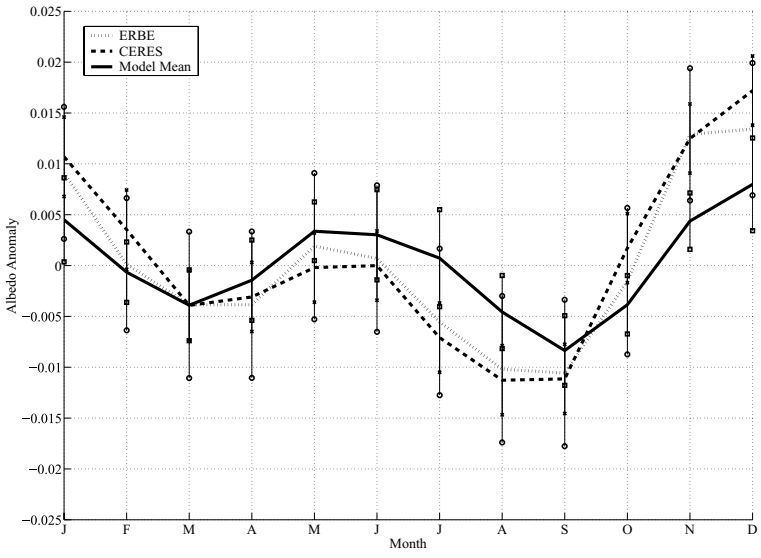

Fig. 3. Average seasonal anomalies for ERBE (February 1985–May 1989), CERES (March 2000–December 2003) and models (February 1985–Decemeber 2003). The solid line represents the mean of all 20 models, with error bars marked with squares indicating one standard deviation. The error bars on the observational data, marked with crosses and circles for ERBE and CERES, respectively, indicate one standard deviation due to the random error in the measurements.

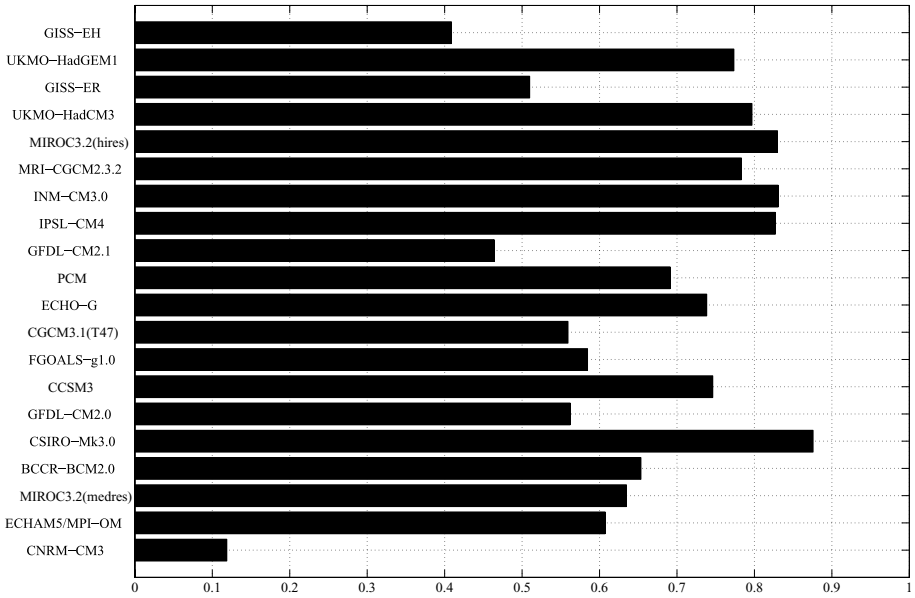

Fig. 4. Correlations between monthly mean albedos in ERBE and 20 models (February 1985–May 1989) time series, seasonal cycle included.

forcings applied, nor feedbacks they may cause, appear to have caused significant trends in albedo over the studied period.

For the observations, 5 and 3 years of data, respectively, is hardly sufficient as a basis for trend analysis, given the large inter-annual variability in the system. Furthermore, instrumental and orbital drift and other technicalities can cause temporal variations that may be mistaken for physical trends.

Given these caveats, the de-seasonalized ERBE data have a negative linear trend of 15×10^{-4} per year. This can be compared to the error estimates given by Wielicki et al. (1995) for a 5-year trend, of 0.3 Wm^{-2}, corresponding to 9.2×10^{-4} for albedo. The change in albedo over the 52-month period is of the same order of magnitude as the estimated error, and could therefore, in a formal sense, be real. The change can also be compared to the earthshine measurements of Earth's reflectivity. Pallé et al. (2004) find a drop in albedo of 0.02 from 1984 to 2000, and this change corresponds to a yearly trend comparable to that seen in the ERBE data. The earthshine indication of an increase in albedo of 0.016 from 2000 to 2004 is not supported by CERES data from this period, as pointed out by Wielicki et al. (2005). (It should be noted that earthshine observations are not truly global.) The trend in the CERES data used here is less than -3×10^{-5} per year, which is well within the precision uncertainty of 9.2×10^{-4} (0.3 Wm^{-2}) for a 5-year trend (Wielicki et al., 1995), and hence not of statistical significance.

As already pointed out (cf. Section 3.1), the difference between ERBE and CERES measurements should not be seen as proof of a physical albedo drop. No more can be said than that 'there may be a real difference between ERBE and CERES SW fluxes', as stated in the online data quality summaries (http://eosweb.larc.nasa.gov).

3.4. Correlations

Figure 4 shows correlations between global monthly mean albedo time series for ERBE and the 20 models. The strong seasonal cycle dominates the correlations between modelled and measured time series. When the time series are de-seasonalized, all models have correlations weaker than 0.5 (not shown), but when the seasonal cycle is included all models except for CNRM-CM3, IPSL-CM4 and GISS-EH have correlations between 0.5 and 0.88. The still-not-perfect correlation is due to differences in seasonal cycle as well as in year-to year variablity and trends.

The correlation at each point in space is not as good as that for the global mean, even when the seasonal cycle is included. Figure 5 shows the geographical distribution of correlation—at each point on the $2.5^\circ \times 2.5^\circ$ ERBE grid—on a global map. The picture shows the mean of all of the modelled correlations with ERBE observations. We consider the use of the model ensemble mean to be sufficient for this purpose, since the patterns are very similar for the individual modelled correlations.

Note that the coverage is only between ca. 66° S and 66° N since the polar areas will not be sun-lit, and albedo thereby not defined, during their respective winter months.

Just like the global means, the geographically specified correlations will be dominated by the level of agreement between the annual cycles in ERBE and the models. For the interpretation of Fig. 5, this means that a high or low correlation mainly represents a well or poorly reproduced seasonal variation. The de-seasonalized correlations are much weaker.

The correlation is seen to increase with increasing latitude, which is to be expected since the seasonal cycle is stronger at higher latitudes. At the mid-latitude storm tracks the correlations

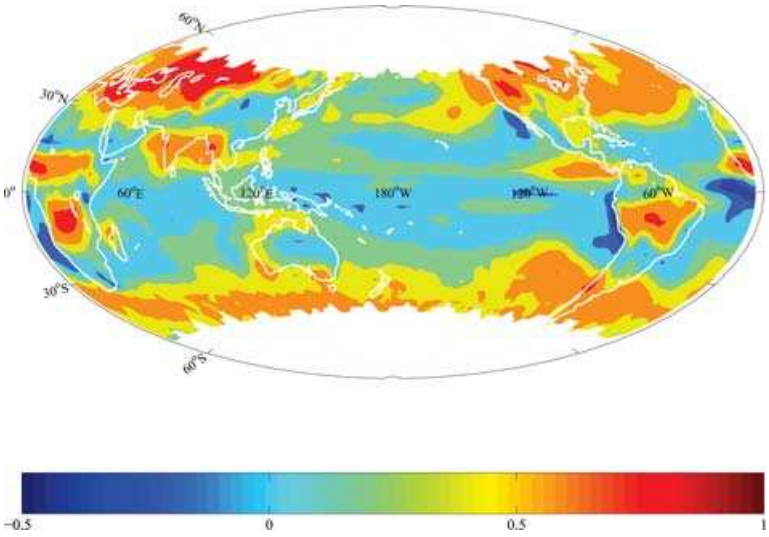

Fig. 5. The mean geographical distribution of correlation between monthly mean albedo in ERBE and 20 GCMs, November 1984–February 1990.

are around and above 0.5, indicating that their annual variation is captured in some sense by the models. There is also indication of the ITCZ over the continents, as well as the monsoon circulation over Asia being well represented in the models. The correlation is generally lower over the oceans, with near zero or even negative correlations. The reflectivity of the ocean surface is sensitive to the solar angle, and it is possible that this sensitivity is not well reproduced by the models. Areas with conspicuously large negative correlations (ca. −0.5) are found at the subtropical west coasts of Africa and North and South America. These regions, dominated by low stratiform clouds over cold ocean currents, are apparently poorly simulated, albedowise, by the models. The poor simulation of clouds in these areas has previously been pointed out by, for example, Weare (2004), and improvement is essential given the significant role they play in determining climate sensitivity and cloud feedback uncertainties (Bony and Dufresne, 2005). Low or negative correlations (0 to −0.5) are also found over Australia, northern Africa and central Asia. These are all dry desert-regions, where the models hence seem to fail to represent the albedo variations correctly.

3.5. Latitude and time dependence of differences

We study the temporal evolution of the model-to-measurement discrepancies by looking at Hovmöller plots of the difference between ERBE and GCM albedos. In Fig. 6, we show the result for MIROC3.2(hires), as an example. This model agrees relatively well with ERBE in the mean-the global mean over the whole ERBE-period (0.298) is only 1% higher than the ERBE mean (0.294), and the correlation with ERBE is 0.83 when the seasonal cycle is included.

Figure 6 shows that the albedo anomalies at specific latitudes and times range from −0.1 to 0.1. All models have a similar range of differences, but the distribution of the anomalies varies. In the case of MIROC3.2(hires), the agreement in absolute values with ERBE is good at low northern latitudes, but tends to deteriorate with latitude, with a strong under-estimation of albedo in the model at ca. 60°N during boreal summer.

In the SH, there is a tendency of over-estimation of albedo in the model from the equator up to around 40°S during austral winter, and bettter agreement during austral summer in this latitude band. Also seen in Fig. 6 is a large re-occurring under-estimation of the albedo during austral summer at ca. 60°S. A pattern similar to this occurs to some extent in almost all the models. (see Appendix A)

Comparing these results to the discussion of annual cycles (cf. Section 3.2), the patterns seen in the SH agree with the general tendency for the mean of the models, including MIROC3.2(hires), to under-estimate the albedo during boreal winter, and over-estimate it during boreal summer. The NH anomalies seem to have less influence on the global seasonal anomalies.

4. Discussion

From our comparison between satellite observations and GCM simulations of the planetary albedo, we find that models and measurements differ in many respects.

GCM-derived albedos are almost consistently higher than the values observed by satellites. For the period with global ERBE data (February 1985–May 1989), the modelled global mean albedo is on average 0.009 above the measured global mean. This corresponds to a difference in radiative flux of almost 3 Wm^{-2}. The mean level of global mean albedo according to CERES (March 2000–December 2003) is an additional ca. 0.012 below the ERBE mean, corresponding to an additional flux difference of ca. 4 Wm^{-2}.

The difference between the two measurement sets may indicate a real albedo difference betweeen the two measurement periods, but part of it is undoubtedly due to calibration and

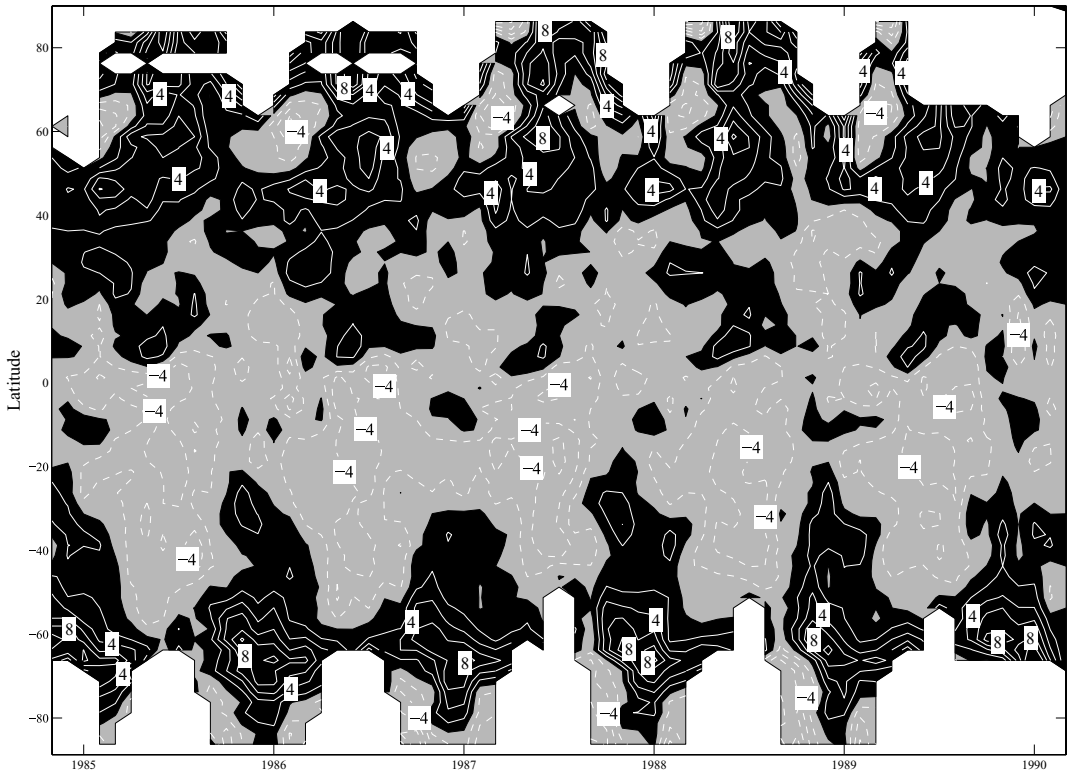

Fig. 6. Difference between ERBE albedo and model albedo, as a function of latitude and time (November 1984–February 1990). Positive anomalies, where ERBE is higher, indicated with black, and negative anomalies, where ERBE is lower, with grey. Numbers are scaled by a factor of 100, so that the contour intervals correspond to 2×10^{-2}, and the contour labels to $\pm 4 \times 10^{-2}$ and $\pm 8 \times 10^{-2}$. (See Appendix A, Fig. 7, for corresponding plots for each of the models.)

algorithm differences. The fact that the models are closer to the ERBE data and farther from the CERES data raises the question of how they are being and should be tuned to satellite measurements.

The models have difficulties capturing the difference between the higher NH winter solstice peak and the lower SH winter solstice peak in the seasonal cycle of albedo, seen in the ERBE and CERES observations. This is likely due to the representation of snow and ice in the models. Large and consistent differences in absolute values between ERBE and model albedos occur at high southern latitudes during boreal summer, where almost all models under-estimate the albedo by as much as 0.1.

The geographical distribution of correlation with ERBE is very similar for all the models. The pattern clearly distinguishes between better and more poorly simulated regions, the agreement between the annual cycles being especially prominent in determining the strength of the correlation. Mid-latitude areas seem to be well represented. Ocean areas are generally worse simulated than continental areas, and subtropical areas dominated by marine low stratocumulus clouds show particularly large disagreement. Other problematic areas identified are dry desert regions in the subtropics, for example, Australia, northern Africa and central Asia, where models also show strong negative correlations with ERBE.

In this study, we have seen that there are substantial differences between models and measurements when it comes to regional and global albedo. By pointing out specific problems and apparent shortcomings, we hope to facilitate the improvement of GCMs in this respect. We have also seen that large uncertainties and poor/insufficient coverage in observations make it hard to draw conclusions with confidence, and we therefore take this opportunity to urge experimentalists to refine their products and quantify the uncertainties therein. Of course development of the two go hand in hand, and by improving both models and measurements we will decrease differences and increase understanding, which is a basic condition for our future attempts to understand climate stability.

5. Acknowledgments

We thank the international modelling groups for providing their data for analysis, the Program for Climate Model Diagnosis and Intercomparison for collecting and archiving the model data, the JSC/CLIVAR Working Group on Coupled Modelling and their Coupled Model Intercomparison Project and Climate

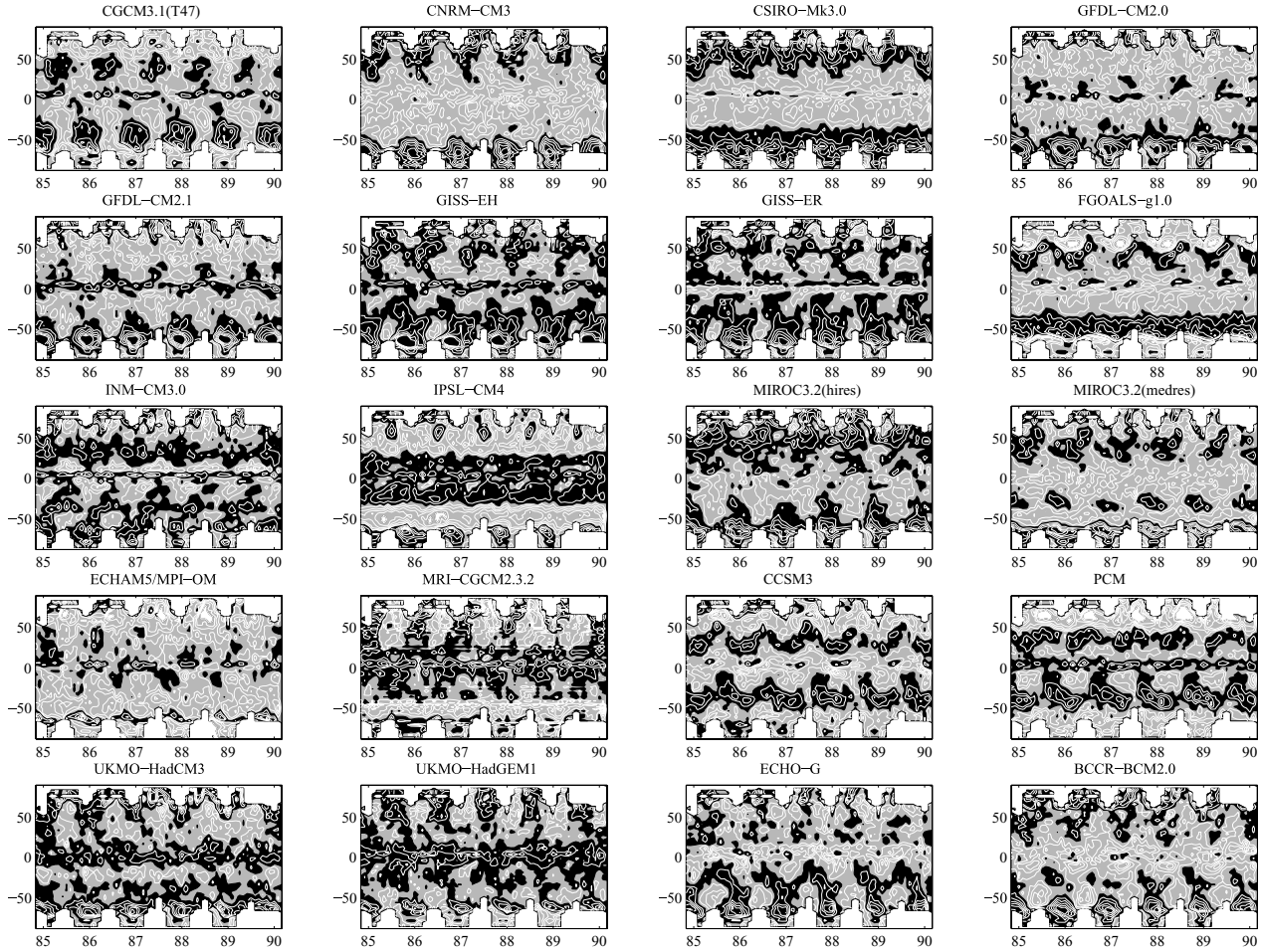

Fig. 7. Difference between ERBE albedo and model albedo, as a function of latitude and time (November 1984–February 1990). Positive anomalies, where ERBE is higher, indicated with black, and negative anomalies, where ERBE is lower, with grey. Contour intervals are 2×10^{-2}.

Simulation Panel for organizing the model data analysis and the IPCC Working Group 1 Technical Support Unit for technical support. The IPCC Data Archive at Lawrence Livermore National Laboratory is supported by the Office of Science, U.S. Department of Energy.

NASA Langley Research Center is acknowledged for data distribution. We are particularly grateful to Takmeng Wong for help with satellite data. Thanks are also due to Tad Anderson, University of Washington, and Johannes Karlsson, Stockholm University, for help of all kinds.

6. Appendix A: Hovmöller plots

Figure 7 shows the temporal evolution, from November 1984 to February 1990, of the zonal mean difference between ERBE and model monthly mean albedo, for each of the 20 GCMs. As mentioned in Section 3.5, the under-estimation of albedo by models during austral summer, at latitudes between ca. 40°S and 80°S reoccurs in almost all models, while most other patterns are not consistent amongst the models.

References

ACIA, 2004. Impacts of a Warming Arctic–Arctic Climate Impact Assessment. Cambridge University Press, Cambridge, 144.

Barkstrom, B. R. 1984. The earth radiation budget experiment (ERBE). *Bull. Amer. Meteor. Soc.* **65**, 1170–1185.

Barkstrom, B. R. and Smith, G. L. 1986. The earth radiation budget experiment: science and implementation. *Rev. Geophys.* **24**, 379–390.

Bony, S. and Dufresne, J.-L. 2005. Marine boundary layer clouds at the heart of tropical cloud feedback uncertainties in climate models. *Geophys. Res. Lett.* **32**, L20806.

Charlson, R. J., Schwartz, S. E., Hales, J. M., Cess, R. D., Coakley, J. A. and co-author, 1992. Climate forcing ny anthropogenic aerosols. *Science* **255**, 423–430.

Chen, T., Rossow, W. B. and Zhang, Y. 2000. Radiative effects of cloud-type variations. *J. Clim.* **13**, 264–286.

Gates, W. L. and Boyle, 1992. AMIP – the Atmospheric Model Intercomparison Project. *Bull. Amer. Meteor. Soc.* **73**, 1962–1970.

Gates, W. L., Boyle, J. S., Dease, C. G., Doutriaux, C. M., Drach, C. M. and co-authors, 1999. An overview of the results of the Atmospheric Model Intercomparison Project (AMIP I). *Bull. Amer. Meteor. Soc.* **80**, 29–55.

Harrison, E. F., Minnis, P., Barkstrom, B. R., Ramanathan, V., Cess, R. D. and co-authors, 1990. Seasonal variation of cloud radiative forcing derived from the earth radiation budget experiment. *J. Geophys. Res.* **95**, 18,687–18,703.

Hartmann, D. L., Ockert-Bell, M. E. and Michelsen, M. L. 1992. The effect of cloud type on earth's energy balance: global analysis. *J. Clim.* **5**, 1281–1304.

IPCC, 2001. Climate Change 2001: The Scientific Basis. Contribution of Working Group I to the Thirs Assessment Report of the Intergovernmental Panel on Climate Change, (eds. J. T. Houghton, Y. Ding, D. J. Griggs, M. Noguer, P. J. van der Linden et al.) Cambridge University Press, Cambridge, United Kingdom, and New York, 881.

Kiehl, J. T., Hack, J. J. and Hurrell, J. W. 1998. The energy budget of the NCAR Community Climate Model: CCM3. *J. Clim.* **11**, 1151–1178.

Loeb, N. G., Smith, N. M., Kato, S., Miller, W. F., Gupta, S. K. and co-authors. 2003. Angular distribution models for top-of-atmosphere radiative flux estimation from the clouds and the Earth's Radiant Energy System instrument on the Tropical Rainfall Measuring Mission Satellite. Part I: Methodology. *J. Appl. Meteor.* **42**, 240–265.

Loeb, N. G., Kato, S., Loukachine, K. and Manalo-Smith, N. 2005. Angular distribution models for top-of-atmosphere radiative flux estimation from the clouds and the Earth's radiant energy system instrument on the Terra satellite. Part I: methodology. *J. Atmos. Ocean. Tech.* **22**, 338–351.

Moberg, A., Sonechkin, D. M., Holmgren, K., Datsenko, N. M. and Karlén, W. 2005. Highly variable Northern Hemisphere temperatures reconstructed from low- and high-resolution proxy data. *Nature* **433**, 613–617.

Norris, J. R. 2005. Multi-decadal changes in near-global cloud cover and eztimated cloud cover radiative forcing. *J. Geophys. Res.* **110**, D08206.

Pallé, E., Goode, P. R., Montañés-Rodríguez, P. and Koonin, S. E. 2004. Changes in the Earth's reflectance over the past two decades. *Science* **304**, 1299–1301.

Potter, G. L. and Cess, R. D. 2004. Testing the impact of clouds on the radiation budgets of 19 atmospheric general circulation models. *J. Geophys Res.* **109**, D02106.

Ramanathan, V., Cess, R. D., Harrison, E. F., Minnis, P., Barkstrom, B. R. and co-authors, 1989. Cloud-radiative forcing and climate: Results from the Earth Radiation Budget Experiment. *Science* **243**, 57–63.

Roeckner, E., Schlese, U., Biercamp, J and Loewe, P. 1987. Cloud optical depth feedbacks and climate modelling. *Nature* **329**, 138–140.

Santer, B. D., Wigley, T. M.L., Mears, C., Wentz, F. J., Klein, S. A. and co-authors, 2005. Amplification of surface temperature trends and variability in the tropical atmosphere. *Science* **309**, 1551–1556.

Smith, G. L., Wielicki, B. A., Barkstrom, B. R., Lee, R. B., Priestly, K. J. and co-authors, 2004. Clouds and the Earth radiant energy system: an overview. *Advances in Space Research* **33**, 1125–1131.

Weare, B. C. 2004. A comparison of AMIP II model cloud layer properties with ISCCP D2 estimates. *Climate Dyn.* **22**, 281–292.

Wielicki, B.A, Cess, R. D., King, M. D., Randall, D. A. and Harrison, E. F. 1995. Mission to Planet Earth: role of Clouds and radiation in climate. *Bull. Amer. Meteor. Soc.* **76**, 2125–2153.

Wielicki, B. A., Barkstrom, B. R., Harrison, E. F., Lee, R. B. III, Smith, L. and co-authors, 1996. Clouds and the Earth's radiant energy system (CERES): an Earth observing system experiment. *Bull. Amer. Meteor. Soc.* **77**, 853–868.

Wielicki, B. A., Wong, T., Allan, R. P., Slingo, A., Kiehl, J. and co-authors, 2002. Evidence for large decadal variability in the tropical mean radiative energy budget. *Science* **295**, 841–844.

Wielicki, B. A., Wong, T., Loeb, N., Minnis, P., Priestly, K. and co-authors, 2005. Changes in Earth's albedo measured by satellite. *Science* **308**, 825–825.